Acta Mech Sin (2008) 24:285–288
DOI 10.1007/s10409-008-0146-1

RESEARCH PAPER

Material and structural instabilities of single-wall carbon nanotubes

J. Wu · K. C. Hwang · J. Song · Y. Huang

Received: 27 November 2007 / Revised: 7 December 2007 / Accepted: 7 December 2007 / Published online: 6 March 2008

Abstract The nonlinear atomistic interactions usually involve softening behavior. Instability resulting directly from this softening are called the material instability, while those unrelated to this softening are called the structural instability. We use the finite-deformation shell theory based on the interatomic potential to show that the tension instability of single-wall carbon nanotubes is the material instability, while the compression and torsion instabilities are structural instability.

Keywords Carbon nanotubes · Instability

1 Introduction

Single-wall carbon nanotubes (SWCNT's) display superior mechanical, thermal and electrical properties, and have many applications in nanotechnology. They have been modeled as linear elastic thin shells with the Young's modulus E and shell thickness h fitted by the atomistic simulation results of tension and bending rigidities. Specifically, the thickness h is obtained from

$$h = \sqrt{12 \frac{\text{bending rigidity}}{\text{tension rigidity}}} \tag{1}$$

based on the classical linear elastic shell theory. Such an approach, however, leads to large scattering of shell thickness [1–11], which gives the Young's modulus varying by an order of magnitude, known as the "Yakobson's paradox" [12].

Huang et al. [11] explained the Yakobson's paradox. Without any parameter fitting, they determined analytically the tension, shear, bending and torsion rigidities directly from the interatomic potential for carbon [13,14]. For a graphene, which is the limit of SWCNT's with the radii approaching infinity, the torsion rigidity vanishes, while other rigidities do not. These give

$$\frac{\text{bending rigidity}}{\text{tension rigidity}} \neq \frac{\text{torsion rigidity}}{\text{shear rigidity}}, \tag{2}$$

since its right-hand side equals zero, and its left-hand side does not vanish and defines the SWCNT shell thickness as in Eq. (1). This inequality contradicts the classical linear elastic plate theory [15], which gives the same ratio of bending/tension and torsion/shear rigidities. It is responsible for the aforementioned scattering of shell thickness in the continuum shell modeling of SWCNT's because the thickness thus defined depends on the loading. For example, the pure twisting $\kappa_{11} = -\kappa_{22}$ and $\kappa_{12} = 0$ gives zero thickness, while the equ-biaxial bending $\kappa_{11} = \kappa_{22}$ and $\kappa_{12} = 0$ gives a non-vanishing thickness.

Wu et al. [16] established a finite-deformation shell theory directly from the interatomic potential for carbon [13,14]. This atomistic-based continuum shell theory accounts for the nonlinear, mutli-body atomistic interactions, as well as the effect of SWCNT chirality, without any parameter fitting. Wu et al. [17] then studied the instability of SWCNT's subjected

J. Wu · K. C. Hwang
FML, Department of Engineering Mechanics,
Tsinghua University, Beijing 100084, China

J. Song
Department of Mechanical Science and Engineering,
University of Illinois, 1206 W. Green Street,
Urbana, IL 61801, USA

Y. Huang (✉)
Department of Civil and Environmental Engineering and
Department of Mechanical Engineering, Northwestern University,
Evanston, IL 60208, USA
e-mail: y-huang@northwestern.edu

to different loadings. The critical strain for instability in tension is around 30%, while the critical strain for compression and twist for torsion are small, and depend strongly on the SWCNT length. The present paper does not account for the Stone–Wales transformation (5775 defect), which may occur prior to tension instability [18].

The nonlinear atomistic interactions always involve softening at large deformation. The instability results directly from this softening is called the material instability, while the instability unrelated to this softening (e.g., Euler buckling) is called the structural instability. The purpose of this paper is to determine whether the tension, compression and torsion instabilities of SWCNT's are material or structural instabilities. The paper is structured as follows. The constitutive model for the atomistic-based finite-deformation shell theory [16] is briefly reviewed in Sect. 2. An SWCNT subjected to tension/compression and torsion is studied in Sects. 3 and 4, respectively. The strains at which the applied loads reach the maximum, or equivalently the tangent rigidities vanish are then compared to the critical strains for bifurcation [17] in order to determine whether they are material and structural instabilities.

2 Constitutive model for the finite-deformation shell theory based on the interatomic potential

The Green strain tensor and curvature tensor in the SWCNT are denoted by $\boldsymbol{E}$ and $\boldsymbol{K}$, respectively. The strain energy density W is an analytic function of $\boldsymbol{E}$ and $\boldsymbol{K}$ obtained from the interatomic potential [16]. The second Piola–Kirchhoff stress tensor $\boldsymbol{T}$ and bending moment tensor $\boldsymbol{M}$ are work conjugates of $\boldsymbol{E}$ and $\boldsymbol{K}$,

$$\boldsymbol{T} = \frac{\partial W}{\partial \boldsymbol{E}}, \quad \boldsymbol{M} = \frac{\partial W}{\partial \boldsymbol{K}}. \tag{3}$$

Their increments are related by

$$\begin{aligned} \dot{\boldsymbol{T}} &= \boldsymbol{L} : \dot{\boldsymbol{E}} + \boldsymbol{H} : \dot{\boldsymbol{K}}, \\ \dot{\boldsymbol{M}} &= \boldsymbol{H}^{\mathrm{T}} : \dot{\boldsymbol{E}} + \boldsymbol{S} : \dot{\boldsymbol{K}}, \end{aligned} \tag{4}$$

where $\boldsymbol{L} = \boldsymbol{L}^{\mathrm{T}}$ and $\boldsymbol{S} = \boldsymbol{S}^{\mathrm{T}}$ are the symmetric tension and bending rigidity tensors given analytically in terms of the interatomic potential, $\boldsymbol{H}$ and its transpose $\boldsymbol{H}^{\mathrm{T}}$ are the coupled tension/bending rigidity tensors.

The results presented in the following are based on the Brenner potential for carbon [13].

3 Tension/compression

For an armchair or zig-zag SWCNT of radius R subjected to simple tension/compression, the deformation is uniform prior to instability. A material point $\boldsymbol{P} = R\boldsymbol{e}_R + Z\boldsymbol{e}_Z$ on the SWCNT prior to deformation moves to $\boldsymbol{p} = R(1 + \varepsilon_{\mathrm{lateral}})\boldsymbol{e}_R + Z(1 + \varepsilon_{\mathrm{axial}})\boldsymbol{e}_Z$ after the deformation, where $\varepsilon_{\mathrm{axial}}$ is the axial strain, and $\varepsilon_{\mathrm{lateral}}$ is the strain in circumferential direction to be determined in terms of $\varepsilon_{\mathrm{axial}}$.

The non-vanishing components of the Green strain and curvature tensors are

$$\begin{aligned} E_{\Theta\Theta} &= \varepsilon_{\mathrm{lateral}} + \frac{1}{2}\varepsilon_{\mathrm{lateral}}^2, \\ E_{ZZ} &= \varepsilon_{\mathrm{axial}} + \frac{1}{2}\varepsilon_{\mathrm{axial}}^2, \\ K_{\Theta\Theta} &= -R^{-1}\varepsilon_{\mathrm{lateral}}. \end{aligned} \tag{5}$$

The non-vanishing components of the second Piola–Kirchhoff stress and bending moment tensors are

$$\begin{aligned} T_{\Theta\Theta} &= \frac{\partial W}{\partial E_{\Theta\Theta}}, \qquad T_{ZZ} = \frac{\partial W}{\partial E_{ZZ}}, \\ M_{\Theta\Theta} &= \frac{\partial W}{\partial K_{\Theta\Theta}}, \qquad M_{ZZ} = \frac{\partial W}{\partial K_{ZZ}}. \end{aligned} \tag{6}$$

The equilibrium equation in the current configuration becomes

$$T_{\Theta\Theta} - \frac{M_{\Theta\Theta}}{R(1 + \varepsilon_{\mathrm{lateral}})} = 0, \tag{7}$$

which determines $\varepsilon_{\mathrm{lateral}}$ in terms of $\varepsilon_{\mathrm{axial}}$. The total axial force on the SWCNT is

$$F = 2\pi R(1 + \varepsilon_{\mathrm{axial}})T_{ZZ}. \tag{8}$$

The tangent rigidity of the SWCNT in tension/compression is defined by

$$C_{\mathrm{Tension}} = \frac{\dot{F}}{d_{zz}}, \tag{9}$$

where $d_{zz} = \dfrac{\dot{\varepsilon}_{\mathrm{axial}}}{1 + \varepsilon_{\mathrm{axial}}}$ is the rate of deformation. Figure 1 shows the tangent rigidity C_{Tension}, normalized by the circumference $2\pi R$ of the undeformed SWCNT versus the axial strain $\varepsilon_{\mathrm{axial}}$ for the armchair (8,8) and zig-zag (14,0) SWCNT's subjected to uniaxial tension and compression. The critical strains for bifurcation obtained by Wu et al. [17] are also shown by the solid and open circles in Fig. 1. For the armchair (8,8) SWCNT in tension, bifurcation always occurs once the tangent rigidity reaches zero regardless of the SWCNT length. For the zig-zag (14,0) SWCNT in tension, bifurcation depends on the SWCNT length, and occurs after the tangent rigidity reaches zero and becomes negative, i.e., the bifurcation corresponds to softening in atomistic interactions. This is somewhat similar to plastic shear localization in plasticity [19], which also occurs in the softening stage. Therefore, the bifurcation of SWCNT's in tension represents the material instability.

For SWCNT's in compression, bifurcation depends on the SWCNT length, and occurs when the tangent rigidity is still

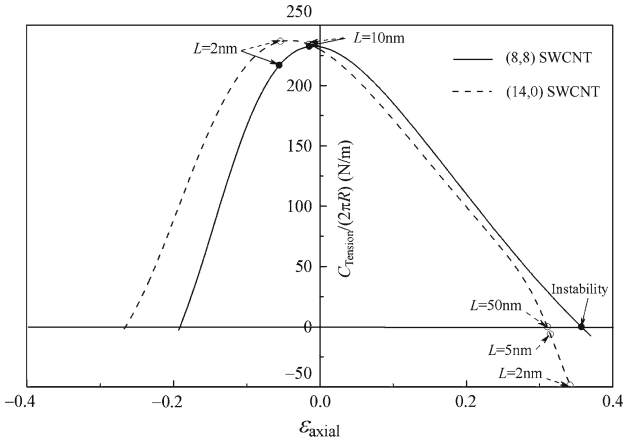

Fig. 1 The tangent rigidities of armchair (8,8) and zig-zag (14,0) single-wall carbon nanotubes, normalized by the nanotube circumference $2\pi R$, versus the (nominal) axial strain. The *solid* and *open circles* denote the critical bifurcation strains for different nanotube length L

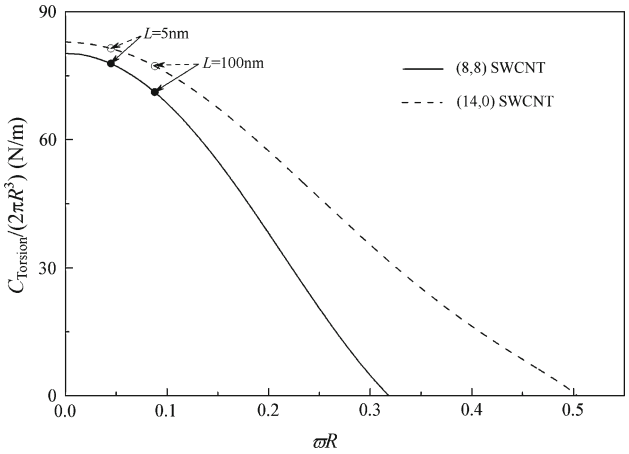

Fig. 2 The tangent rigidities of armchair (8,8) and zig-zag (14,0) single-wall carbon nanotubes, normalized by $2\pi R^3$, versus the nominal twist, where R is the radius of undeformed nanotube. The *solid* and *open circles* denote the critical twist for bifurcation for different nanotube length L

positive. This suggests that bifurcation in compression corresponds to structural instability. In fact, the bifurcation mode [17] is the same as the Euler buckling for long SWCNT's.

4 Torsion

For an armchair or zig-zag CNT of radius R subjected to torsion, the deformation is uniform prior to instability. Let ϖ denote the twist (rotation per unit length). A material point $\boldsymbol{P} = R\boldsymbol{e}_R + Z\boldsymbol{e}_Z$ on the CNT prior to deformation moves to $\boldsymbol{p} = R(1+\varepsilon_{\text{lateral}})(\boldsymbol{e}_R\cos\varpi Z + \boldsymbol{e}_\Theta \sin\varpi Z) + Z(1+\varepsilon_{\text{axial}})\boldsymbol{e}_Z$ after the deformation, where the axial strain $\varepsilon_{\text{axial}}$ and the strain $\varepsilon_{\text{lateral}}$ in the circumferential direction are to be determined in terms of ϖ.

The components of the Green strain and curvature tensor are

$$\begin{aligned} E_{\Theta\Theta} &= \varepsilon_{\text{lateral}} + \frac{1}{2}\varepsilon_{\text{lateral}}^2, \\ E_{ZZ} &= \varepsilon_{\text{axial}} + \frac{1}{2}\varepsilon_{\text{axial}}^2 + \frac{1}{2}\varpi^2 R^2(1+\varepsilon_{\text{lateral}})^2, \\ E_{\Theta Z} &= \frac{1}{2}\varpi R(1+\varepsilon_{\text{lateral}})^2, \end{aligned} \tag{10}$$

$$\begin{aligned} K_{\Theta\Theta} &= -R^{-1}\varepsilon_{\text{lateral}}, \\ K_{ZZ} &= -\varpi^2 R(1+\varepsilon_{\text{lateral}}), \\ K_{\Theta Z} &= -\varpi(1+\varepsilon_{\text{lateral}}). \end{aligned} \tag{11}$$

The components of second Piola–Kirchhoff stress and bending moment tensors are

$$T_{\Theta\Theta} = \frac{\partial W}{\partial E_{\Theta\Theta}}, \quad T_{ZZ} = \frac{\partial W}{\partial E_{ZZ}}, \quad T_{\Theta Z} = \frac{\partial W}{\partial E_{\Theta Z}}, \tag{12}$$

$$M_{\Theta\Theta} = \frac{\partial W}{\partial K_{\Theta\Theta}}, \quad M_{ZZ} = \frac{\partial W}{\partial K_{ZZ}}, \quad M_{\Theta Z} = \frac{\partial W}{\partial K_{\Theta Z}}. \tag{13}$$

The equilibrium equations in the current configuration become

$$T_{\Theta\Theta} + 2\varpi R T_{\Theta Z} - \frac{M_{\Theta\Theta} + 2\varpi R M_{\Theta Z} + \varpi^2 R^2 M_{ZZ}}{R(1+\varepsilon_{\text{lateral}})} = 0, \tag{14}$$

$$T_{ZZ} = 0, \tag{15}$$

which give $\varepsilon_{\text{axial}}$ and $\varepsilon_{\text{lateral}}$ in terms of ϖ. The torque on the SWCNT is

$$\begin{aligned} M_{\text{Torsion}} = 2\pi R(1+\varepsilon_{\text{lateral}})[&R(1+\varepsilon_{\text{lateral}}) \\ &\times(T_{\theta Z} + \varpi R T_{ZZ}) - 2(M_{\theta Z} + \varpi R M_{ZZ})]. \end{aligned} \tag{16}$$

The tangent rigidity of SWCNT in torsion is defined by

$$C_{\text{Torsion}} = \frac{\dot{M}_{\text{Torsion}}}{(1+\varepsilon_{\text{axial}})^{-1}\dot{\varpi}}. \tag{17}$$

Figure 2 shows the tangent rigidity C_{Torsion} normalized by $2\pi R^3$ versus the normalized twist ϖR for the armchair (8,8) and zig-zag (14,0) SWCNT's subjected to pure torsion. The critical strains for bifurcation obtained by Wu et al. [17] are also shown by the solid and open circles in Fig. 2. Bifurcation clearly depends on the SWCNT length, and occurs when the tangent rigidity is still positive, which suggests that the bifurcation in torsion corresponds to structural instability.

5 Concluding remarks

The bifurcation of single-wall carbon nanotubes in tension are due to softening in the atomistic interactions, i.e., material instability. The bifurcations in compression and torsion

are not due to softening in the atomistic interactions, i.e., structural instability, which is similar to Euler buckling.

Acknowledgments Y. Huang acknowledges the support from ONR Composites for Marine Structures Program (grant N00014-01-1-0205, Program Manager Dr. Y. D. S. Rajapakse). K.C. Hwang acknowledges the supports from the National Basic Research Program of China (973 Program, 2007CB936803). The authors also acknowledge the supports from the NSFC and Ministry of Education of China.

References

1. Pantano, A., Parks, D.M., Boyce, M.C.: Nonlinear structural mechanics based modeling of carbon nanotube deformation. Phys. Rev. Let. **91**, 145504 (2004)
2. Yakobson, B.I., Brabec, C.J., Bernholc, J.: Nanomechanics of carbon tubes: instabilities beyond linear response. Phys. Rev. Lett. **76**, 2511–2514 (1996)
3. Lu, J.P.: Elastic properties of carbon nanotubes and nanoropes. Phys. Rev. Lett. **79**, 1297–1300 (1997)
4. Zhou, X., Zhou, J.J., Ou-Yang, Z.C.: Strain energy and Young's modulus of single-wall carbon nanotubes calculated from electronic energy-band theory. Phys. Rev. B **62**, 13692 (2000)
5. Kudin, K.N., Scuseria, G.E., Yakobson, B.I.: C2F, BN, and C nanoshell elasticity from ab initio computations. Phys. Rev. B **64**, 235406 (2001)
6. Odegard, G.M., Gates, T.S., Nicholson, L.M., Wise, K.E.: Equivalent-continuum modeling of nano-structured materials. Comp. Sci. Technol. **62**, 1869–1880 (2002)
7. Jin, Y., Yuan, F.G.: Simulation of elastic properties of single-walled carbon nanotubes. Comp. Sci. Technol. **63**, 1507–1515 (2003)
8. Vodenitcharova, T., Zhang, L.C.: Effective wall thickness of a single-walled carbon nanotube. Phys. Rev. B **68**, 165401 (2003)
9. Goupalov, S.V.: Continuum model for long-wavelength phonons in two-dimensional graphite and carbon nanotubes. Phys. Rev. B **71**, 085420 (2005)
10. Wang, L., Zheng, Q., Liu, J.Z., Jiang, Q.: Size dependence of the thin-shell model for carbon nanotubes. Phys. Rev. Lett. **95**, 105501 (2005)
11. Huang, Y., Wu, J., Hwang, K.C.: Thickness of graphene and single-wall carbon nanotubes. Phys. Rev. B **74**, 245413 (2006)
12. Shenderova, O.A., Zhirnov, V.V., Brenner, D.W.: Carbon nanostructures. Crit. Rev. Solid State Mater. Sci. **27**, 227–356 (2002)
13. Brenner, D.W.: Empirical potential for hydrocarbons for use in simulating the chemical vapor deposition of diamond films. Phys. Rev. B **42**, 9458–9471 (1990)
14. Brenner, D.W., Shenderova, O.A., Harrison, J.A., Stuart, S.J., Ni, B., Sinnott, S.B.: A second-generation reactive empirical bond order (REBO) potential energy expression for hydrocarbons. J. Phys. Condens. Matter **14**, 1783–1802 (2002)
15. Timoshenko, S., Woinowsky-Krieger, S.: Theory of Plates and Shells. McGraw-Hill, New York (1959)
16. Wu, J., Hwang, K.C., Huang, Y.: An atomstic-based finite-deformation shell theory for single-wall carbon nanotubes. J. Mech. Phys. Solids **56**, 279–292 (2008). doi:10.1016/j.jmps.2007.05.008
17. Wu, J., Hwang, K.C., Song, J., Huang, Y.: A finite-deformation shell theory for carbon nanotubes based on the interatomic potential. Part II: instability analysis. J. Appl. Mech. (Accepted)
18. Jiang, H., Feng, X.Q., Huang, Y., Hwang, K.C., Wu, P.D.: Defect nucleation in carbon nanotubes under tension and torsion: Stone-Wales transformation. Comput. Methods Appl. Mech. Eng. **193**, 3419–3429 (2004)
19. Rice, J.R.: The localization of plastic deformation. In: Koiter, W.T. (ed.) Theoretical and Applied Mechanics, pp. 207–220. North-Holland, Amsterdam (1976)